Inorg. Chem. **2003**, *42*, 6379–6387

Intramolecular Electrocatalysis of 8-Oxo-Guanine Oxidation: Secondary Structure Control of Electron Transfer in Osmium-Labeled Oligonucleotides

Rebecca C. Holmberg,[†] Mark T. Tierney,[‡] Patricia A. Ropp,[†] Eric E. Berg,[†] Mark W. Grinstaff,*[,‡] and H. Holden Thorp*[,†]

Department of Chemistry, The University of North Carolina at Chapel Hill, Chapel Hill, North Carolina 27599-3290 and Department of Chemistry, Duke University, Durham, North Carolina 27708

Received January 6, 2003

A phosphoramidite containing $Os(bpy)_3^{2+}$ (**Os**; bpy, 2,2′-bipyridine) with a three-carbon linker was synthesized and used to prepare oligonucleotides with the **Os** redox catalyst appended to the 5′-end. The electrogenerated Os(III) is capable of oxidizing 7,8-dihydro-8-oxo-guanine (**8G**), but 8G is not electrochemically reactive at indium tin oxide electrodes because of poor electrode kinetics for the direct reaction. The hairpin-forming oligonucleotide **Os**-5′-ATG TCA GAT TAG CAG GCC TGA CAT **8G** was synthesized and characterized by thermal denaturation and native gel electrophoresis both in the hairpin form and when hybridized to its Watson–Crick complement. The redox potential in both forms of the appended Os(III/II) couple was 0.63 V (all potentials vs Ag/AgCl), which is identical to that for the free complex. The diffusion coefficients of the hairpin form (10.2×10^{-7} cm^2/s) and the duplex form (8.7×10^{-7} cm^2/s) were consistent with values expected from studies of noncovalently bound redox labels, which suggest that the measured diffusion coefficient should be that of the appended DNA molecule. The oligonucleotide was designed such that in the duplex form, the **8G** is far from the Os(III/II) couple, but in the hairpin form, the **8G** is situated close to the redox center. For the duplex form, cyclic voltammetry studies showed that mediated oxidation of the **8G** nucleobase occurred only through bimolecular reaction of the electrogenerated Os(III) of one duplex with the **8G** of another duplex. However, in the hairpin form, intramolecular electron transfer from **8G** to Os(III) *in the same molecule* was apparent in both chronoamperometry and cyclic voltammetry.

Introduction

The macromolecular structure of biomolecules allows for the incorporation of multiple redox sites into spatially controlled locations.[1−4] In enzymes, such architectures lead to vectorial charge transport and direction of reducing or oxidizing equivalents into desired substrates. A common feature of such systems is a difference in the electron-transfer self-exchange rates for the different redox partners. For example, common redox enzyme systems incorporate catalytic cofactors in buried sites and redox mediators on the surface of the protein.[5] Typically, the redox mediator sites undergo rapid electron transfer while the catalytic sites are sluggish. Such a design allows for the electrons to flow always through the redox mediator and not inadvertently into the catalytic site.

The ability of DNA to mediate charge transfer between remote sites has been a subject of intense interest.[6−10] There is now considerable agreement that electrons (or oxidizing

* Author to whom corrspondence should be addressed. E-mail: holden@unc.edu.
[†] University of North Carolina.
[‡] Duke University.

(1) Rack, J. J.; Krider, E. S.; Meade, T. J. *J. Am. Chem. Soc.* **2000**, *122*, 6287−6288.
(2) Grinstaff, M. W. *J. Inorg. Biochem.* **2001**, *86*, 53−53.
(3) Reichert, D. E.; Lewis, J. S.; Anderson, C. J. *Coord. Chem. Rev.* **1999**, *184*, 3−66.
(4) Bjerrum, M. J.; Casimiro, D. R.; Chang, I. J.; Dibilio, A. J.; Gray, H. B.; Hill, M. G.; Langen, R.; Mines, G. A.; Skov, L. K.; Winkler, J. R.; Wuttke, D. S. *J. Bioenerg. Biomembr.* **1995**, *27*, 295−302.
(5) Lippard, S. J. In *Bioinorganic Chemistry*; Bertini, I., Gray, H. B., Lippard, S. J., Valentine, J. S., Eds.; University Science: Mill Valley, CA, 1994; pp 505−584.
(6) Berlin, Y. A.; Burin, A. L.; Ratner, M. A. *J. Am. Chem. Soc.* **2001**, *123*, 260−268.
(7) Barnett, R. N.; Cleveland, C. L.; Joy, A.; Landman, U.; Schuster, G. B. *Science* **2001**, *294*, 567−571.

10.1021/ic030004f CCC: $25.00
Published on Web 09/11/2003

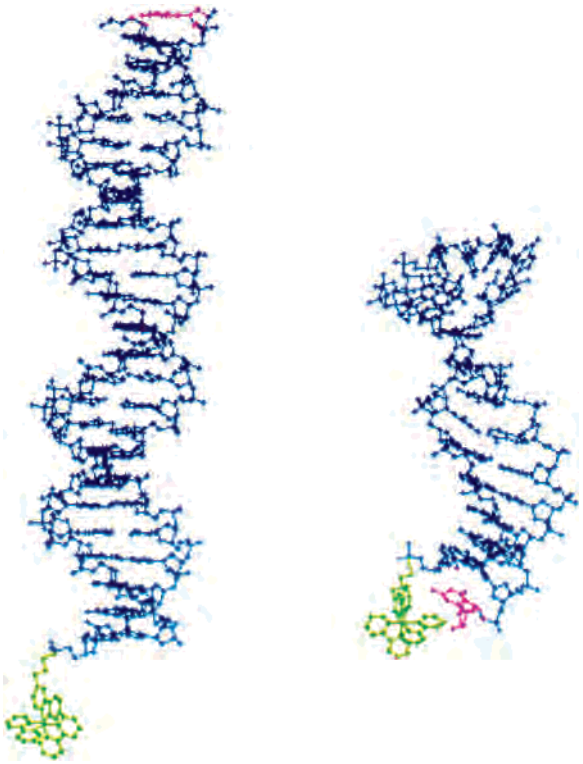

Figure 1. HyperChem model of double-stranded (**3·2**) vs single-stranded (**3**) **Os**-modified oligonucleotide. Oligonucleotide scaffold (blue), **8G** (purple), **Os** (green).

equivalents) are transferred over relatively long distances in duplex DNA when the energetics of the reaction permit the intermediacy of oxidized nucleobases between the donor and acceptor, leading to an electron-hopping mechanism.[8] When the energies of the donor and acceptor are not suitable for creating an oxidized site in the bridge, electron transfer proceeds via conventional tunneling over moderate distances.[8]

Here we report on a simple system for studying conformationally controlled electron transfer in DNA molecules using electrochemistry. The design of the system is shown in Figure 1. The electron-transfer molecule consists of a 25-mer oligonucleotide labeled with $Os(bpy)_3^{2+}$ (**Os**; bpy, 2,2′-bipyridine) on one end and 7,8-dihydro-8-oxo-guanine (**8G**) on the other. As we have shown previously, $Os(bpy)_3^{2+}$ is a good oxidant for **8G** when electrochemically oxidized to the Os(III) state so that catalytic currents are observed for the Os(III/II) couple in the presence of **8G**.[11] However, when the tethered system is hybridized to its Watson−Crick complement, the Os(III) is too far from the **8G** for electron transfer to occur, particularly since the energy of the Os(III) is too low to generate intervening nucleobase radicals that would be required to realize efficient charge separation over such a long distance. In addition, indium tin oxide (ITO) is a kinetically poor oxidant for nucleobases,[12] so no direct oxidation of **8G** is detectable. In the absence of the complementary strand, the labeled strand forms a hairpin where **8G** is now in close proximity to the Os(III) and electron transfer is apparent as a catalytic current in the cyclic voltammetry. The osmium center therefore acts as a catalyst for the electrochemical oxidation of **8G**.

Experimental Section

1. Os-Labeled Oligodeoxynucleotide Synthesis. a. Materials. All reagents were purchased from Aldrich at the highest purity. All solvents were purchased from Fisher. 8-oxo-dG modified CPG (500 Å) DNA synthesis columns were purchased from Chemgenes. All other DNA synthesis reagents and supplies were purchased from Glen Research. All solvents were dried and freshly distilled prior to use. 4-Methyl-2,2′-bipyridine was prepared according to the literature procedure.[13] $Os(bpy)_2Cl_2$ was prepared by previously reported procedures.[14] Reverse phase (RP) high-performance liquid chromatography (HPLC) was performed on a Rainin HPLC with a C18 column monitoring at 254 nm. NMR spectra were recorded on a Varian INOVA spectrometer operating at 400 MHz or a GE QE-300 spectrometer operating at 300 MHz. Fast atom bombardment mass spectra (FAB-MS) were obtained on a JEOL JMS-SX102A spectrometer using a 3-nitrobenzyl alcohol matrix. Matrix-assisted laser desorption ionization time-of-flight (MALDI-TOF) mass spectra of oligodeoxynucleotides were obtained using a PerSeptive Biosystems Voyager-DE biospectrometry workstation operating in the positive ion mode using a hydroxypicolinic acid matrix.

b. 4-[3-(*tert*-Butyl-dimethyl-silanyloxy)-propyl]-[2,2′]bipyridine (A). To a solution of freshly distilled diisopropylamine (0.043 g, 0.42 mmol) in THF (10 mL) at −78 °C was added *n*-butyllithium (0.17 mL of a 2.5 M solution in cyclohexane, 0.42 mmol). The solution was allowed to warm to room temperature over 1 h. Next, the mixture was cooled to −78 °C. 4-Methylbipyridine (0.060 g, 0.35 mmol) was added, and the mixture was allowed to stir for 0.5 h. 2-(*tert*-Butyldimethylsiloxy)-bromoethane (0.101 g, 0.353 mmol) was then added, and the mixture was allowed to warm to room temperature. The mixture was stirred for an additional 3 h, poured into 5 mL of 10% citric acid, and extracted with ethyl acetate (3 × 50 mL). The ethyl acetate solution was washed with water (15 mL) and brine (100 mL). The solution was dried over Na_2SO_4, and the solvent was removed. Column chromatography over silica gel (pretreated with triethylamine, 89:10:1 hexane/CH_2Cl_2/TEA) yielded a colorless oil (0.102 g, 88%). ^{1}H NMR ($CDCl_3$): δ 8.61 (ddd, 1H, J = 6.61, 1.71, 0.86 Hz), 8.49 (d, 1H, J = 4.95 Hz), 8.33 (dt, 1H, J = 8.03, 0.85 Hz), 8.20 (d, 1H, 0.86 Hz), 7.72 (dt, 1H, J = 7.69, 1.71), 7.21 (ddd, 1H, 7.35, 4.79, 1.20 Hz), 7.08 (dd, 1H, J = 4.96, 1.54 Hz), 3.58 (t, 2H, J = 6.15 Hz), 2.71 (t, 2H, J = 7.69 Hz), 1.84 (m, 2H), 0.84 (s, 9H), −0.02 (s, 6H). ^{13}C NMR: δ 156.14, 155.84, 148.96, 148.92, 136.18, 123.97, 123.50, 121.12, 61.96, 33.18, 31.68, 25.84, 18.19, −5.42. Electron impact high-resolution mass spectrometry (EI-HRMS) calcd for $C_{19}H_{28}ON_2Si$, 328.1971 $(M)^+$; found, 328.1966.

c. 3-[2,2′]Bipyridinyl-4-yl-propan-1-ol (B). To a solution of **A** (0.095 g, 0.290 mmol) in THF (5 mL) was added 10% aqueous HCl (1 mL). The reaction was stirred vigorously for 14 h. Next,

(8) (a) Giese, B. *Annu. Rev. Biochem.* **2002**, *71*, 51−70. (b) Wan, C.; Fiebig, T.; Schiemann, O.; Barton, J. K.; Zewail, A. H. *Proc. Natl. Acad. Sci. U. S. A.* **2000**, *97*, 14052−14055.
(9) Nunez, M. E.; Hall, D. B.; Barton, J. K. *Chem. Biol.* **1999**, *6*, 85−97.
(10) Lewis, F. D.; Kalgutkar, R. S.; Wu, Y. S.; Liu, X. Y.; Liu, J. Q.; Hayes, R. T.; Miller, S. E.; Wasielewski, M. R. *J. Am. Chem. Soc.* **2000**, *122*, 12346−12351.
(11) Ropp, P. A.; Thorp, H. H. *Chem. Biol.* **1999**, *6*, 599−605.
(12) Armistead, P. M.; Thorp, H. H. *Anal. Chem.* **2001**, *73*, 558−564.
(13) Savage, S. A.; Smith, A. P.; Fraser, C. L. *J. Org. Chem.* **1998**, *63*, 10048−10051.
(14) Kober, E. M.; Caspar, J. V.; Sullivan, B. P.; Meyer, T. J. *Inorg. Chem.* **1980**, *27*, 4587−4598.

saturated $NaHCO_3$ was added (10 mL) and the mixture was extracted with ethyl acetate (4 × 50 mL). The organic phase was washed with water (100 mL) and brine (100 mL) and dried with Na_2SO_4. Column chromatography (basic alumina, 2% MeOH in CH_2Cl_2) afforded the product as a colorless oil (0.45 g, 73%). ^{1}H NMR ($CDCl_3$): δ 8.59 (dt, 1H, J = 4.78, 0.85), 8.48 (d, 1H, J = 4.95 Hz), 8.31 (dd, 1H, J = 7.60, 0.85 Hz), 8.16 (d, 1H, 0.68 Hz), 7.75 (dt, 1H, J = 6.65, 1.37 Hz), 7.23 (dd, 1H, J = 8.20, 4.78 Hz), 7.08 (dd, 1H, J = 4.78, 1.37 Hz), 3.60 (t, 2H, J = 6.32 Hz), 3.10 (br, 1H), 2.73 (t, 2H, J = 7.52 Hz), 1.84 (m, 2H). ^{13}C NMR: δ 156.03, 155.77, 149.00, 148.91, 137.01, 124.01, 123.65, 121.30, 61.32, 32.92, 31.52. FAB-HRMS calcd for $C_{13}H_{15}ON_2$, 215.1184 $(M + H)^+$; found, 215.1182.

d. [Bis-(4,4′-bipyridine)]-[3-[2,2′]bipyridinyl-4-yl-propan-1-ol]osmium(II) Hexafluorophosphate (C). $Os(bpy)_2Cl_2$ (0.96 g, 0.17 mmol) and bipyridine alcohol **B** (0.40 g, 0.19 mmol) were heated to reflux for 2 h. The mixture was cooled, added to a concentrated solution of NH_4PF_6(aq), and cooled to 5 °C for 14 h. Following filtration, the resulting solid was washed with cold water and dried. Next, the solid was dissolved in a minimum amount of CH_3CN (~3 mL) and precipitated in ether to afford the product after filtration (0.153 g, 81%). ^{1}H NMR (CD_3COCD_3): δ 8.81−8.74 (m, 5H), 8.67 (d, 1H, J = 1.6 Hz), 8.00−7.89 (m, 10H), 7.76 (d, 1H, 5.6 Hz), 7.47−7.41 (m, 5H), 7.35 (dd, 1H, J = 5.8, 1.6 Hz), 3.56 (t, 2H, J = 6.4 Hz), 2.97 (t, 2H, J = 7.6 Hz), 2.81 (br, 1H), 1.87 (m, 2H). FAB-MS 863 $(M - PF_6)^+$, 718 $(M - 2PF_6)^+$. FAB-HRMS calcd for $C_{33}H_{30}ON_6OsPF_6$, $(M - PF_6)^+$ 863.1738; found, 863.1757.

e. [Bis-(4,4′-bipyridine)]-[diisopropyl-phosphoramidous acid 3-[2,2′]bipyridinyl-4-yl-propyl ester 2-cyano-ethyl ester]osmium-(II) Hexafluorophosphate (D). To a solution of alcohol C (0.113 g, 0.112 mmol) in CH_3CN was added diisopropylethylamine (0.022 g, 0.167 mmol). Next, β-cyanoethyl-diisopropylchlorophosphoramidite (0.032 g, 0.134 mmol) was added slowly dropwise to the gently stirring mixture. The mixture was stirred until thin layer chromatography showed complete conversion of the starting material. MeOH was added (2 drops), and most of the solvent was removed under reduced pressure. A degassed mixture of ether and hexanes (1:1) was added, causing the separation of the product. The mixture was decanted and the residue washed with additional degassed ether/hexanes. The residue was dried extensively under vacuum. A sample was checked by ^{31}P NMR, and the remainder was dissolved to a concentration of 0.1 M (based on starting material) with acetonitrile and loaded on an automated DNA synthesizer. These operations were carried out under inert atmosphere with minimal exposure to light. ^{31}P NMR: 148.00, 149.95.

f. Oligodeoxynucleotide Syntheses. Oligodeoxynucleotide syntheses were performed on a commercial ABI 395 DNA synthesizer from the 3′ to 5′ end using standard automated DNA synthesis protocols according to previously published procedures (1.0 mmol scale).[15−17] A 0.1 M solution of phosphoramidite in dry acetonitrile was prepared and installed on the DNA synthesizer in a standard reagent bottle. Normal solid-phase oligodeoxynucleotide synthesis was performed. In the last step, the osmium phosphoramidite was introduced and allowed to react with the oligodeoxynucleotide for 5 min. Redox-labeled oligodeoxynucleotides were deprotected in 30% ammonium hydroxide at 55 °C for 16 h.

(15) Tierney, M. T.; Grinstaff, M. W. J. *Org. Chem.* **2000**, *65*, 5355−5359.
(16) Hu, X.; Lee, S. J.; Grinstaff, M. W. In *Redox Cell Biology and Genetics, Part B*, Sen, C. K., Packer, L., Eds.; Academic Press: San Diego, CA, 2002; Vol. 353, pp 548−566.
(17) Khan, S. I.; Beilstein, A. E.; Sykora, M.; Smith, G. D.; Hu, X.; Grinstaff, M. W. *Inorg. Chem.* **1999**, *38*, 3922−3925.

Table 1. Oligonucleotide Sequences

oligonucleotides	sequence (5′−3′)
control	
1	ATG TCA GAT TAG CAG GCC TGA CAT (**8G**) G[a]
2	ATG TCA GGC CTG CTA ATC TGA CAT
Os conjugated	
3	**Os**-ATG TCA GAT TAG CAG GCC TGA CAT (**8G**)
4	**Os**-ATG TCA GAT TAG CAG GCC TGA CAT G

[a] The control oligonucleotide **1** has an extra G on the 3′ end due to difficulty in solid phase synthesis with **8G** as the starting nucleotide. Synthesis of **3** required a specially made column for the synthesis.

g. HPLC Purification and Characterization of the Oligodeoxynucleotides. HPLC purification of the modified oligodeoxynucleotides was accomplished on a Rainin HPLC instrument equipped with a UV detector. RP chromatography was performed on a C18 column (25 cm × 4.6 mm) with acetonitrile (ACN) and 0.1 M aqueous triethylamine acetate (TEAA) as eluting solvents. A flow rate of 3 mL/min was used, and the concentration of ACN was increased from 5 to 38% over 35 min. The retention times of the modified oligodeoxynucleotides were well separated from the unmodified oligodeoxynucleotide products (>2 min). MALDI-TOF mass spectra confirmed formation of the desired modified oligonucleotides (**3**: calcd, 8499; found, 8496. **4**: calcd, 8484; found, 8484).

h. Unlabeled Oligonucleotides. The sequences of the oligonucleotides used in this study are given in Table 1. Unlabeled synthetic oligonucleotides **1** and **2** were purchased from the Lineberger Comprehensive Cancer Center Nucleic Acids Core Facility and purified by gel electrophoresis on a 20% polyacrylamide gel with 7 M urea (Mallinckrodt). Water was purified with a MilliQ purification system (Millipore). Buffer salts were purchased from Mallinckrodt.

i. Sample Preparation. Solution concentrations of metal complex or DNA were determined by spectrophotometry using a Cary 300 Bio UV−vis scanning spectrophotometer. Extinction coefficients used with absorbance measurements in water were ϵ_{486} = 10 864 M^{-1} cm^{-1} for the **Os** oligonucleotide and ϵ_{490} = 12 900 M^{-1} cm^{-1} for $Os(bpy)_3^{2+}$. Unmodified oligonucleotide strand concentrations were determined by absorbance at 260 nm with an extinction coefficient calculated using the nearest-neighbor approximation.[18] Double-stranded oligonucleotide solutions were prepared by mixing a 1:1.2 ratio of the guanine-containing strand and its Watson−Crick complementary strand in sodium phosphate buffer (50 mM NaP_i, 800 mM NaCl, pH 7), heating at 90 °C for 5 min, and cooling to room temperature over 2 h. Hairpin oligonucleotide solutions were prepared in the same manner in the absence of the complementary strand.

2. Nondenaturing Gel Electrophoresis. Single-stranded oligonucleotide was 5′ radiolabeled using γ^{32}P-ATP (New England Nuclear). A 25-μL solution containing 1 μL of single-stranded oligonucleotide (5 μM), 5 μL of Forward Reaction Buffer (5×), 1 μL of γ^{32}P-ATP, 1 μL of T4 Polynucleotide Kinase (Life Technologies), and 17 μL of MilliQ H_2O was heated in a water bath at 37 °C for 20 min. T4 Polynucleotide Kinase was deactivated by heating the reaction solution at 65 °C for 10 min. The ^{32}P-labeled oligonucleotide (diluted to 50 μL) was then purified on a MicroSpin G-50 column (Amersham Pharmacia Biotech). The resulting ^{32}P-labeled oligonucleotide was ethanol precipitated and resuspended in MilliQ water (~400K cts/5 μL). The oligonucleotide was hybridized (in high ionic strength buffer, 50 mM NaP_i, 800 mM

(18) Fasman, G. D. M. M. *Handbook of Biochemistry and Molecular Biology, Section B;* CRC Press: Clevland, OH, 1976; Vol. I.

Scheme 1 [a]

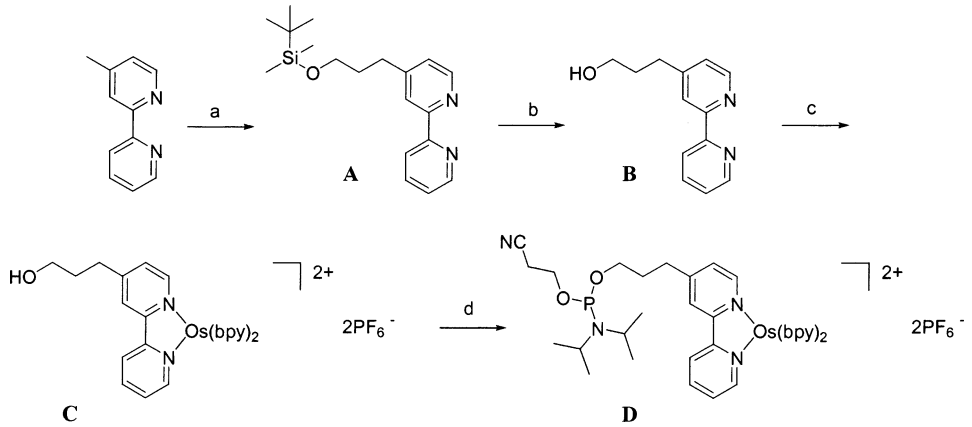

[a] Reagents and Conditions: (a) (1) LDA, THF, −78 °C, (2) $TBDMSOCH_2CH_2Br$, − 78 °C, 88%; (b) 10% HCl (aq), THF, 73%; (c) (1) $Os(bpy)_2Cl_2$, ethylene glycol, reflux, (2) NH_4PF_6, 81%; (d) chloro-2-cyanoethyldiisopropylaminophosphoramidite, DIEA, CH_3CN.

NaCl, pH 7; low ionic strength buffer, 50 mM NaP_i, pH 7) to its complement (added in 10% excess) using 5 μM stock solutions of unlabeled strand. Strands were annealed by heating at 90 °C for 5 min and cooling to room temperature over 2 h (slow-cool) or placing immediately on ice (snap-cool). The samples were then run on a 20% polyacrylamide nondenaturing gel at 250 V for 8 h at 4 °C. The gel was then wrapped and transferred to a phosphorimaging screen and exposed overnight. The gel was scanned on a Storm 840 system phosphorimager (Molecular Dynamics). ImageQuant was used to view and analyze the resulting data.

3. Thermal Denaturation. Thermal denaturation experiments were performed on a Cary 300 Bio UV−vis spectrophotometer. The unlabeled oligonucleotide **1** (4 μM) was annealed in 800 mM NaCl and 50 mM sodium phosphate, pH 7, either alone to form the hairpin or with its complement **2** to form the duplex **1·2** by heating to 95 °C for 5 min and slowly cooling to room temperature over 2 h. By use of the thermal melting program, the temperature of the cell containing the quartz cuvette was preheated to 95 °C and then ramped from 95 to 25 °C and from 25 to 95 °C at 0.5 °C/min while the absorbance at 260 nm was measured every 0.5 °C. The data were smoothed at 0.5 °C intervals with a filter of 5, and the derivative of the resulting curve was taken at a data interval of 0.5 °C to determine T_m.

4. Electrochemistry. ITO electrodes were obtained from Delta Technologies, LTD (Stilwater, MN). All ITO electrodes were cleaned in a four-step sonication process involving an aqueous solution of Alconox, 2-propanol, and two washes with Milli-Q water (6 min each). Electrodes were then dried in an oven (90 °C) for 5 min. The freshly cleaned electrodes were used within 24 h. All electrochemistry was performed in 800 mM NaCl, 50 mM sodium phosphate buffer, pH 7, using a Ag/AgCl reference electrode and Pt-wire counter electrode, ITO area = 0.15 cm^2.

a. Chronoamperometry. Chronoamperometry experiments were performed on a BAS 100B/W potentiostat controlled by a PC. Electrodes were preconditioned by sweeping the potential from 0.0 to 0.95 V a minimum of 5 times at 100 mV/s. The potential was stepped from 400 to 825 mV in the sample solution to minimize double-layer charging effects. The pulse width was 600 ms with a wait time of 5 s. Solutions with 200 μM **Os** oligonucleotide were used to determine the diffusion coefficient of **4** (with and without **2**), and 75 μM solutions were used for experiments containing the modified **8G**.

b. Cyclic Voltammetry. Cyclic voltammetry (CV) experiments were performed on an EG&G PAR 273A potentiostat controlled by a PC. For cyclic voltammetry experiments, the electrode potential was scanned between 0.0 and 0.95 V. Each electrode was electrochemically conditioned prior to data collection by scanning the buffer solution at the intended scan rate (usually seven cycles). The background CV of sodium phosphate buffer was subtracted from the subsequent metal and DNA CV data files before analysis. Cyclic voltammograms of 25, 50, and 75 μM metal-derivatized oligonucleotide in the presence and absence of the reactive nucleobase, **8G**, were recorded for each experiment.

Results and Discussion

Oligonucleotide Characterization. The single-stranded oligonucleotide sequence **3** was designed with **8G** as the first base on the 3′ end and $Os(bpy)_3^{2+}$ (**Os**) attached to the phosphate terminus of the 5′ end (Figure 1). The osmium metal complex was covalently linked to the oligonucleotide via a three-carbon spacer. The modified oligonucleotide was synthesized using phosphoramidite chemistry (Scheme 1) and solid-phase synthesis.[17] When the complementary strand **2** is hybridized to **3**, the DNA duplex (**3·2**) forms a rigid rod separating the osmium complex at one end from the **8G** at the other. However, in the absence of the complementary strand, the two ends of the sequence are complementary to each other and the strand folds back on itself to form a hairpin structure where the **Os** complex is close enough to oxidize the **8G** via a unimolecular electron-transfer event.

To study the effects of the different structural conformations on electron transfer, it was first important to verify that the designed sequence formed the predicted secondary structure. The secondary structures of the designed oligonucleotides were confirmed via nondenaturing gel electrophoresis and thermal denaturation studies of the un-metallo-labeled oligonucleotides **1** and **1·2**. As shown in Figure 2, the double-stranded form **1·2** and the faster-moving hairpin **1** were readily distinguished. The bands observed at both 800 mM NaCl (lanes 1−6) and 0 mM NaCl (lanes 7−12) are of equal intensity, indicating that the structure formation and stability are independent of ionic strength. Only one faster-moving band was observed for both slow-cooled and snap-cooled single-stranded oligonucleotide, demonstrating that the intramolecular hairpin is extremely stable.

Thermal denaturation experiments yielded typical reversible melting curves for both the double-stranded and hairpin

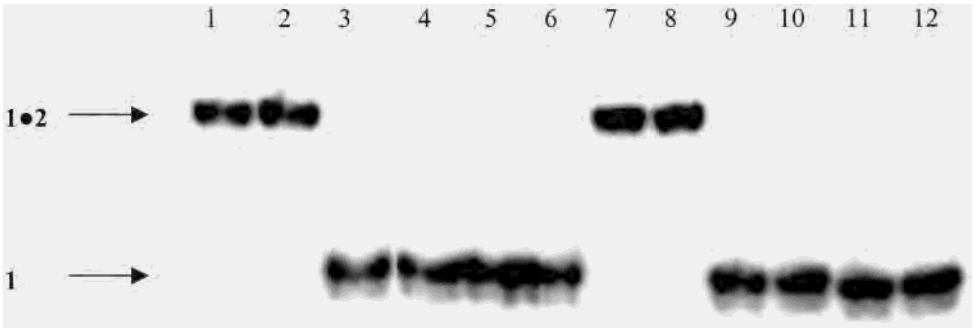

Figure 2. Nondenaturing polyacrylamide gel of **1**, single-stranded and in the presence of **2**: (lanes 1 and 2) **1·2**, high ionic strength (800 mM NaCl, 50 mM sodium phosphate, pH 7); (lanes 3 and 4) **1**, high ionic strength (slow cooled); (lanes 5 and 6) **1**, high ionic strength (snap cooled); (lanes 7 and 8) **1·2**, low ionic strength (50 mM sodium phosphate, pH 7); (lanes 9 and 10) **1**, low ionic strength (slow cooled); (lanes 11 and 12) **1**, low ionic strength (snap cooled).

oligonucleotides. The derivative of the melting curve gave a T_m for **1·2** of 81.3 ± 0.6 °C, very close to the predicted temperature of 81.5 °C for a 24 base pair duplex at the same ionic strength.[19] The observed melting temperature for the hairpin structure was 61.8 ± 0.4 °C, also very similar to the predicted T_m of 61.0 °C from the m-fold program, which predicts thermodynamic properties and secondary structures for single-stranded oligonucleotides under similar conditions.[20] Thus, the melting temperatures strongly suggest that the proper secondary structures of the double-stranded and hairpin conformation form as predicted. This condition was further tested using nondenaturing gel electrophoresis of **1** and an oligonucleotide with the same base composition as **1** but with the nucleotides scrambled to avoid formation of a hairpin (gel given in Supporting Information). This experiment showed that the scrambled **1** ran more slowly than **1** and that both sequences ran identically (and more slowly) when hybridized to their respective complements. This experiment more strongly suggests that **1** forms a hairpin that runs faster than a single strand of identical base sequence. In all cases, only one species was detected on the gel, suggesting that the hairpin form of **1** is not in equilibrium with other structures. The metal-conjugated oligonucleotides are expected to behave in a fashion similar to the underivatized oligonucleotides, since previous studies have shown that the melting temperature is not significantly affected by the covalent attachment of a metal complex with the same tethering group.[16,17,21,22]

Determination of Electrochemical Properties. Oxidation potentials and diffusion coefficients have not been previously reported for these metallo-labeled oligonucleotides. For these studies, we synthesized a labeled oligonucleotide without an **8G** at the 3′ end (**4**) so that the **8G**-Os(III) electron transfer would not obscure the Os(III/II) couple. The redox potential for **4**, measured against an $Fe(CN)_6^{3-}$ standard using a Ag pseudoreference electrode, was determined to be 0.63 ± 0.01 V and was identical for both the hairpin (**4**) and the double-stranded (**4·2**) species. This potential is within error of the known redox potential for $Os(bpy)_3^{2+/3+}$ (0.62 V vs Ag/AgCl).[14] The carbon chain tail extending off of the bipyridine ligand therefore does not considerably affect the redox potential of the metal complex (similar to other reported redox-labeled oligonucleotides).[1]

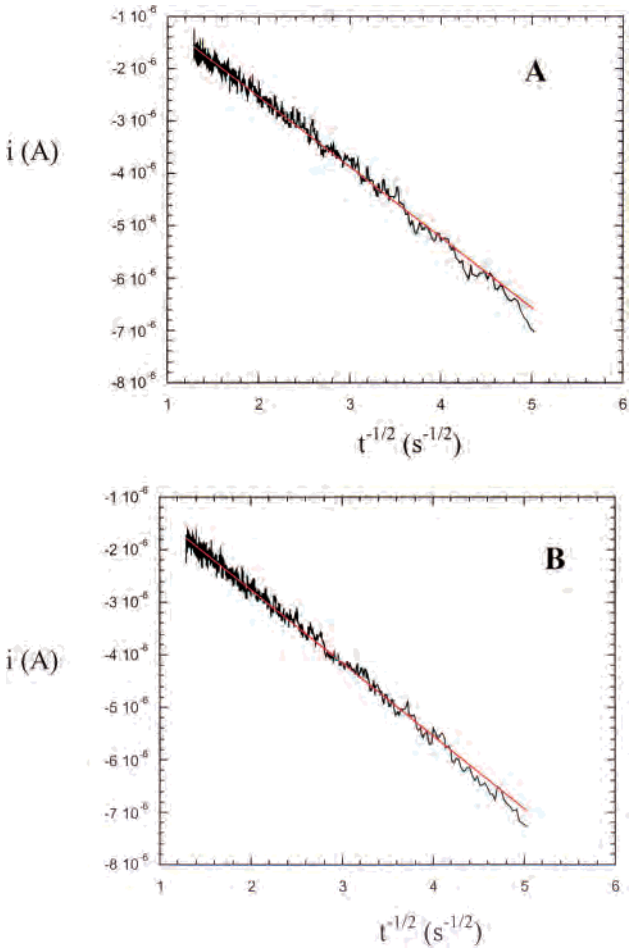

Figure 3. Chronoamperometry experiments for diffusion coefficient determination: (A) **4·2**, slope = -1.35×10^{-6} A $s^{1/2}$, R = 0.994, A = 1.42 cm^2, **4·2** = 185 μM; (B) **4**, slope = 1.44×10^{-6} A $s^{1/2}$, R = 0.995, A = 0.147 cm^2, **4** = 180 μM. Run in 800 mM NaCl, 50 mM NaP_i, pH 7.

Diffusion coefficients have been determined for metal complexes and nucleic acids separately;[23−26] however, the

(19) Blake, R. D.; Delcourt, S. G. *Nucleic Acids Res.* **1998**, *26*, 3323−3332.
(20) Zuker, M. *Nucleic Acids Res.* **2003**, *31*, 1−10. http://www.bioinfo.rpi.edu/applications/mfold/old/dna/form1.cgi.
(21) Khan, S. I.; Beilstein, A. E.; Tierney, M. T.; Sykora, M.; Grinstaff, M. W. *Inorg. Chem.* **1999**, *38*, 5999−6002.
(22) Hu, X.; Smith, G. D.; Sykora, M.; Lee, S. J.; Grinstaff, M. W. *Inorg. Chem.* **2000**, *39*, 2500−2504.
(23) Welch, T. W.; Thorp, H. H. *J. Phys. Chem.* **1996**, *100*, 13829−13836.

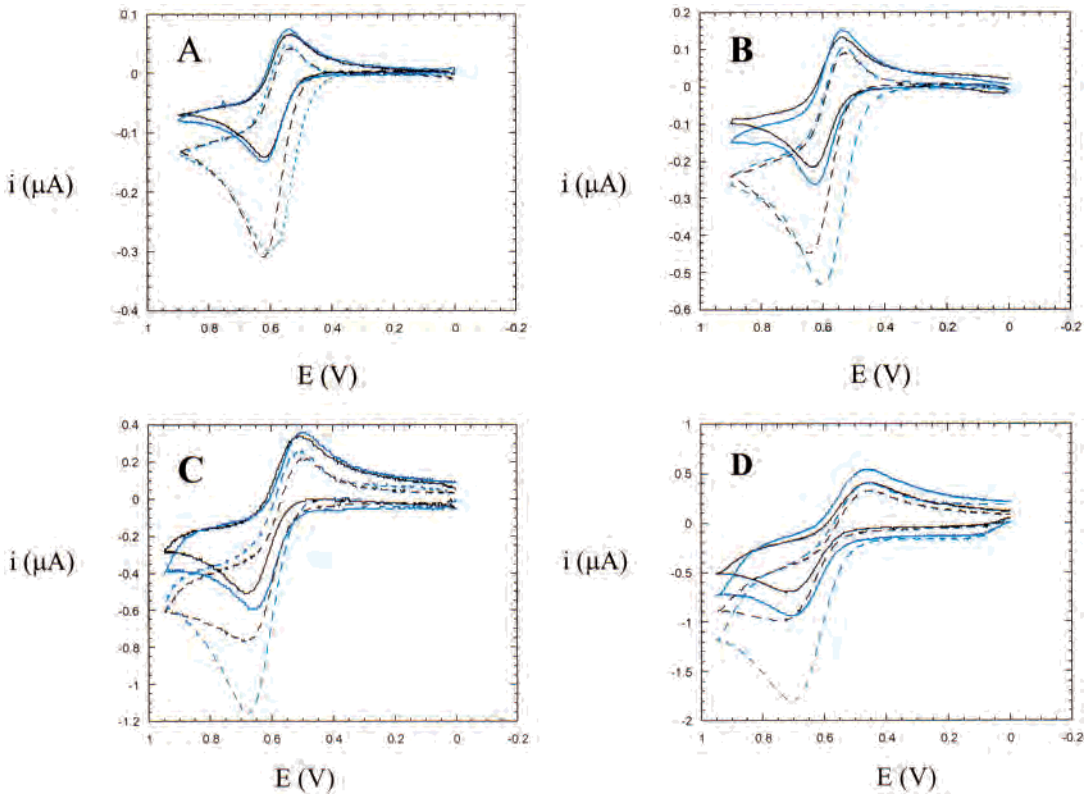

Figure 4. Cyclic voltammograms of 25 μM **3** (dotted) and **4** (solid) in hairpin (blue) and double-stranded (black) conformations at varying scan rates: (A) 25 mV/s, (B) 100 mV/s, (C) 500 mV/s, (D) 1000 mV/s in 800 mM NaCl, 50 mM NaP_i, pH 7.

rate of diffusion of the conjugated metal-nucleic acid species has not been previously studied. We expected that the **Os** label would give a diffusion coefficient similar to that for the much heavier DNA molecule, since intercalating metal complexes exhibit the diffusion coefficient predicted for duplex DNA when bound to the double helix.[24] As expected, the covalent attachment of the oligonucleotide to the osmium metal complex significantly affects the rate of diffusion. The diffusion coefficients for the metallo-labeled oligonucleotides were determined by chronoamperometry (CA) and analyzed using the Cottrell equation[27]

$$i = -nFAD^{1/2}C/\pi^{1/2}t^{1/2} \qquad (1)$$

where n is the number of electrons transferred, F is Faraday's constant in A s/mol, A is the area in cm^2, D is the diffusion coefficient in cm^2/s, and C is the concentration in mol/cm^3. Figure 3 shows a plot of i vs $t^{-1/2}$ for the duplex form (**4·2**) and the hairpin form (**4**). From the slopes of these lines, the diffusion coefficients were $(8.7 \pm 0.2) \times 10^{-7}$ cm^2/s and $(10.2 \pm 0.3) \times 10^{-7}$ cm^2/s, respectively (Table 2); standard deviations are for data taken from three separate trials. These experimentally determined values are much slower than that for free $Os(bpy)_3^{2+}$, which is 73×10^{-7} cm^2/s.[23] Further, the values are in relatively good agreement with the calculated values for 25 and 12 base-pair oligonucleotides as determined from rigid-rod theory (9.43×10^{-7} cm^2/s and 13.0×10^{-7} cm^2/s for the duplex and hairpin forms, respectively).[23,24,28,29] These calculations assume that a rigid rod is formed by the double-stranded nucleic acid and therefore provide only an approximation for the hairpin structure. These values also do not account for the added mass of the Os complex, which might further reduce the diffusion coefficient somewhat. The statistically significant difference in the diffusion coefficients further argues for the desired formation of the hairpin structure.

Table 2. Electrochemical Properties

redox complex	redox potential (V vs Ag/AgCl)	diffusion coefficient[a] (10^{-7}, cm^2 s^{-1})
4	0.63 ± 0.01	10.2 ± 0.3
4·2	0.63 ± 0.01	8.7 ± 0.2
Os	0.62[a]	73[b]

[a] Reference 14. [b] Reference 23.

Electrocatalysis. Having characterized the metal-conjugated oligonucleotide and its designed hairpin and duplex forms, we then studied the electrocatalytic signals in the structures containing the **8G** nucleobase at the opposite end of the metal-linked strand. Both CV and CA were used to monitor the electron transfer. Provided the heterogeneous rate of oxidation of **8G** was much slower than that for Os(III/II),[12] we predicted that there would be faster **8G**−

(24) Welch, T. W.; Corbett, A. H.; Thorp, H. H. *J. Phys. Chem.* **1995**, *99*, 11757−11763.
(25) Carter, M. J.; Bard, A. J. *J. Am. Chem. Soc.* **1987**, *109*, 7528−7530.
(26) Carter, M. T.; Rodriguez, M.; Bard, A. J. *J. Am. Chem. Soc.* **1989**, *111*, 8901.
(27) Bard, A. J.; Faulkner, L. R. *Electrochemical Methods;* John Wiley & Sons, Inc.: New York, 1980.
(28) Tirado, M. M.; Garciadelatorre, J. *J. Chem. Phys.* **1980**, *73*, 1986−1993.
(29) Tirado, M. M.; Martinez, C. L.; Delatorre, J. *G. J. Chem. Phys.* **1984**, *81*, 2047−2052.

Os(III) electron transfer for the hairpin structure **3** where **Os** and **8G** are in close proximity than for the **3·2** duplex where **Os** and **8G** are separated by the rigid DNA duplex. Thus, we expected to observe more catalytic current for the hairpin where **Os** could be oxidized to Os(III) at the electrode and then reduced by **8G**, regenerating Os(II) and establishing a catalytic cycle.[11,30]

Cyclic voltammograms of 25 μM **3** and **4** in both the hairpin (**3** or **4** alone) and double-stranded (**3·2** or **4·2**) conformations were obtained at 25, 100, 500, and 1000 mV/s as shown in Figure 4. At slower scan rates (25 and 100 mV/s, A and B), catalytic current is observed for both **3** and **3·2**. As the scan rate is increased to 500 and 1000 mV/s (C and D), the current from the duplex form steadily decreases while the ratio of catalytic to diffusive current is constant for the hairpin despite the faster sweep rates. Cyclic voltammograms were also obtained at higher concentrations of **3** (50 and 75 μM). At all concentrations, the amount of current from **3** at the fastest sweep rate was double that from **3·2**. This result suggests that Os(II) in **3** (in the hairpin form) can be oxidized a second time following regeneration at the electrode surface after reaction with **8G**, whereas Os(II) in **3·2** is only oxidized once.

The amount of catalytic current was determined as $i_{cat} - i_d$, where the i_{cat} was for the oligonucleotides containing both **8G** and **Os**, and i_d was for the oligonucleotides containing only **Os** but no **8G**. As shown in Figure 5A, the catalytic current from **3·2** levels off at higher scan rates while the current from the hairpin form of **3** continues to increase linearly with square root of scan rate. We do not attempt a quantitative analysis of the electrocatalytic current; the use of a square root axis is simply by convention, since the noncatalytic system should show a square root dependence,[27] as observed. The leveling off of the catalytic current for **3·2** at high scan rates was observed for all of the tested reaction concentrations. As the concentration increases, the current ratio between **3** and **3·2** decreased, presumably due to the higher probability of intermolecular oxidations at higher concentrations (see below).

The reactivities of the hairpin and duplex forms can be understood in terms of two different types of oxidations of **8G** by Os(III): bimolecular, where an Os(III) on one strand oxidizes an **8G** on another strand, and unimolecular, where **8G** is oxidized by the Os(III) on the same strand. Since the two ends of the DNA in the duplex form cannot interact,[28,29] only the bimolecular electron transfer occurs in the duplex form, while both reactions are possible in the hairpin form. The observed trend in the cyclic voltammograms indicates that the contribution of the bimolecular reaction decreases at high scan rates while the unimolecular electron-transfer reaction contributes to the catalytic current at all scan rates for the hairpin form. For the duplex form, the available reaction time at the high scan rates apparently becomes too short for the diffusion-controlled, bimolecular electron transfer to contribute to the catalytic current. In contrast, the

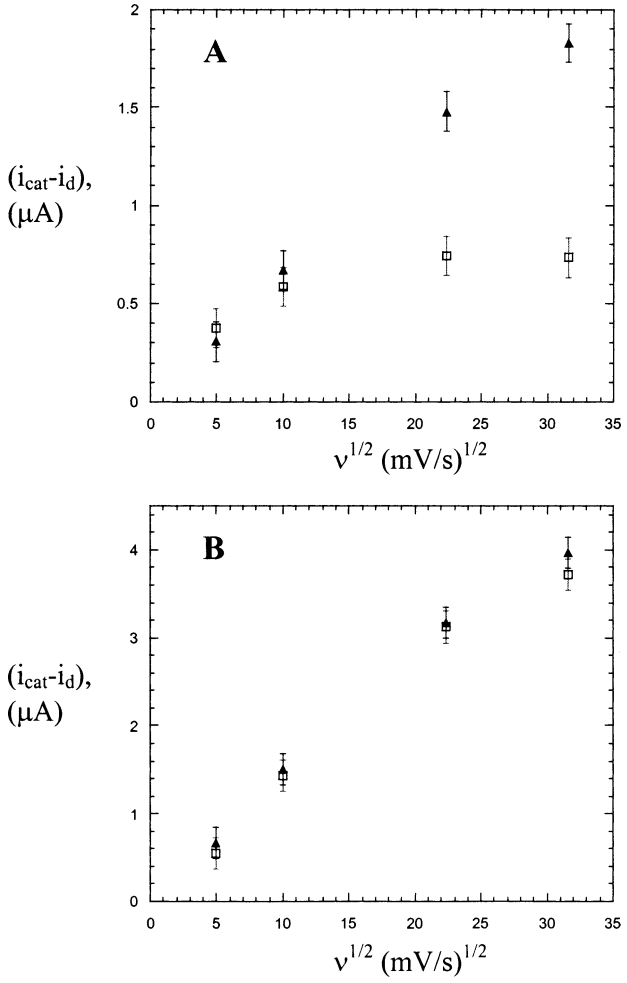

Figure 5. Peak current vs (scan rate)$^{1/2}$: (A) 50 μM **3** (triangles) vs **3·2** (open squares); (B) 50 μM **Os** + 50 μM **1** (triangles) vs 50 μM **Os** + 50 μM **1·2** (open squares) in 800 mM NaCl, 50 mM NaP_i, pH 7.

intramolecular electron transfer in the hairpin form is fast enough to contribute to the catalytic current at the higher scan rates. Of course, bimolecular electron-transfer reactions proceeding in the solution between separate hairpins also contributes to the catalytic current for the hairpin form at low scan rates.

Chronoamperometry experiments support the interpretation of the cyclic voltammetry. Chronoamperograms were obtained for **3** where catalytic current was possible; these were called i_{cat}. The analogous signals for the diffusive-only current in the absence of catalysis, i_d, were obtained by collecting data under identical conditions for oligonucleotide **4**, which does not contain an **8G**. Figure 6 shows the plot of i_{cat} divided by i_d vs the square root of time. For a simple electrocatalytic system with a bimolecular catalytic reaction and an excess of substrate, this plot should give a linear dependence.[27,31] These conditions are not met in our system, since the metal complex and DNA strand are always in a 1:1 ratio.[31] Still, the slopes of the early time points and the time at which the plot levels off offer an assessment of the relative reaction rates for the comparable reactions, as we

(30) Johnston, D. H.; Thorp, H. H. *J. Phys. Chem.* **1996**, *100*, 13837−13843.

(31) Sistare, M. F.; Holmberg, R. C.; Thorp, H. H. *J. Phys. Chem. B* **1999**, *103*, 10718−10728.

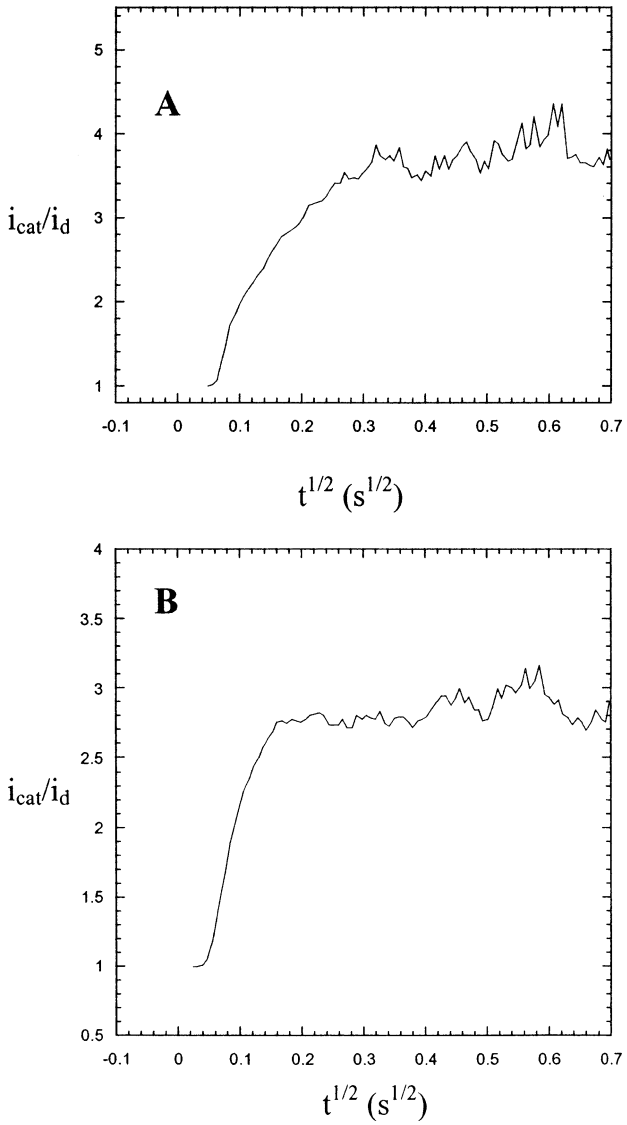

Figure 6. Chronoamperometry experiments for tethered species: (A) 75 μM **3·2**; (B) 75 μM **3** in 800 mM NaCl, 50 mM NaP_i, pH 7.

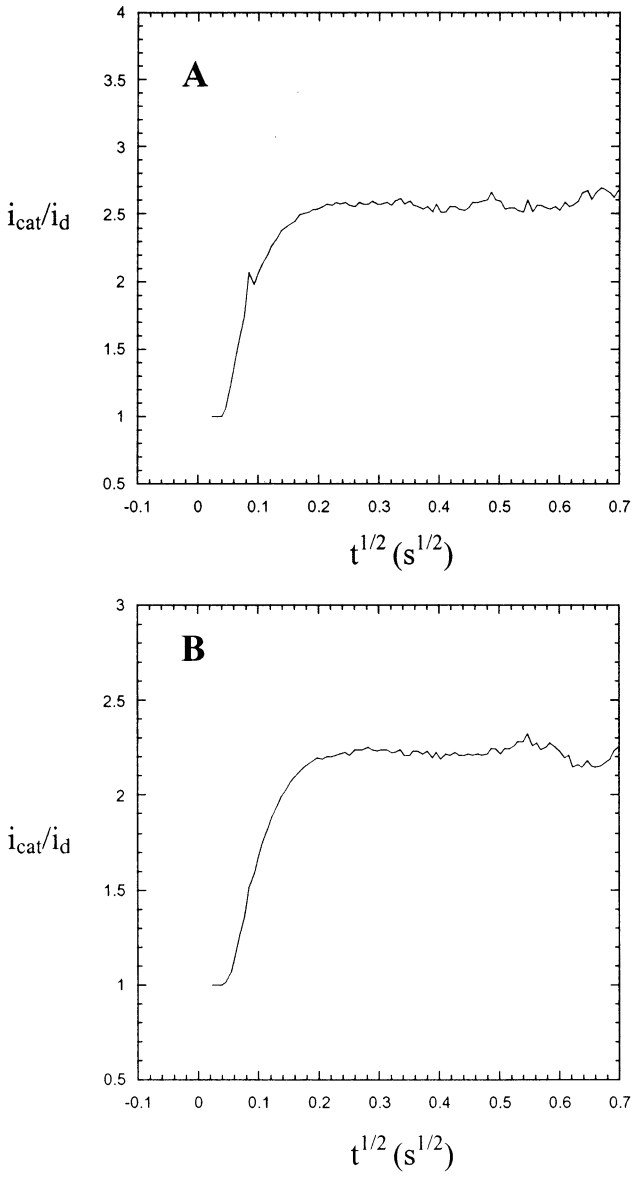

Figure 7. Chronoamperometry experiments for untethered species. (A) 75 μM **Os** + 75 μM **1·2**; (B) 75 μM **Os** + 75 μM **1** in 800 mM NaCl, 50 mM NaP_i, pH 7.

have discussed previously.[31] For both the duplex and hairpin forms, the reaction is over quickly, as indicated by the leveling of the curve. The reaction of **3·2** (Figure 6A) clearly takes much longer to level off than that of the hairpin form of **3** (Figure 6B). This difference in time course supports the analysis of the cyclic voltammetry data. Slightly less overall current is yielded from **3** compared to **3·2**, perhaps due to some degradation resulting from the regenerated electron-transfer event.

Analogous experiments were also performed using free $Os(bpy)_3^{2+}$ in the presence of **1**, which does not have the **Os** label on the 5′ end of the oligonucleotide. These experiments were performed with a 1:1 ratio of $Os(bpy)_3^{2+}$ to oligonucleotide to reflect the relative concentrations of species in the covalently attached forms. As shown in Figure 5B, these cyclic voltammograms exhibit the same amount of catalytic current for both the hairpin and duplex structures, which is consistent with the fact that **8G** is not hydrogen-bonded in either case and that the Os(II) can only be regenerated at the electrode surface once. The same effect was observed at higher concentrations of $Os(bpy)_3^{2+}$ and oligonucleotide. The amount of catalytic current generated by the free $Os(bpy)_3^{2+}$ (Figure 5B) does not decrease as abruptly as the current from **3·2** (Figure 5A) with increasing scan rate, which can be attributed to the larger diffusion coefficient of $Os(bpy)_3^{2+}$ compared to **3·2**. Chronoamperometry experiments were also performed on the solutions of free $Os(bpy)_3^{2+}$ and **1**. Figure 7 shows that the initial slopes from the catalytic reaction of $Os(bpy)_3^{3+}$ with **1·2** and the hairpin form of **1** are similar. This observation confirms that there is no difference in reactivity of the hairpin and duplex forms with unattached $Os(bpy)_3^{2+}$. Furthermore, these results support the conclusion that the difference in catalytic current from **3·2** and the hairpin of **3** is due to the intended geometric constraints on the intramolecular electron transfer and not from a difference in the innate reactivity of **8G** in the two forms.

Conclusions

The ability to site-specifically modify oligonucleotides with redox-active metal complexes has enabled a number of studies of electron transfer across fixed distances in DNA.[1,2,9] These studies have typically been carried out using optical and photochemical methods to monitor the electron transfer.[8,10,32] In contrast, studies of our electrocatalytic system have thus far centered on freely diffusing metal complexes undergoing intermolecular reactions with DNA nucleobases.[11,30,31] Here for the first time, we describe an electrocatalytic system where the metal complex is bound to the oligonucleotide and electrode oxidation of the metal complex leads to *intramolecular* electron transfer from the **8G** nucleobase. The intramolecular electron transfer is apparent through use of a hairpin-forming oligonucleotide that allows for electron transfer in the hairpin form but not in the duplex form. The electron transfer is monitored as excess current in the hairpin forms at high voltammetric sweep rates or at steeper chronoamperometric responses.

The system provides a number of insights. First, tethering the metal complex to the DNA does not perturb the redox potential, and the diffusion coefficient of the covalently attached complex is that of the much larger DNA molecule, as expected from studies of noncovalently bound redox probes.[23−26] Second, electron transfer from **8G** to electrogenerated Os(III) is only observed in the hairpin form where the active nucleobase is close to the metal complex, as expected. These data must be interpreted in light of the intermolecular reaction of Os(III) with an **8G** from a separate DNA molecule, which is apparent at lower sweep rates where sufficient time is available for bimolecular reactions. These studies demonstrate the transferability of the electrocatalytic methodology to metal−DNA conjugates in probing electron transfer in complex biomolecules.

Acknowledgment. We thank Shaun F. Filocamo for a generous gift of 4-methyl-2,2′-bipyridine. R.C.H. thanks the Department of Education for a GAANN-Fellowship.

Supporting Information Available: Nondenaturing gel electrophoresis for **1** and the scrambled sequence. The material is available free of charge via the Internet at http://pubs.acs.org.

IC030004F

(32) Nunez, M. E.; Noyes, K. T.; Gianolio, D. A.; McLaughlin, L. W.; Barton, J. K. *Biochemistry* **2000**, *39*, 6190−6199.